Structural Engineering and Mechanics, Vol. 33, No. 3 (2009) 285-306
DOI: http://dx.doi.org/10.12989/sem.2009.33.3.285

Topology optimization of the structure using multimaterial inclusions

Ryszard Kutyłowski†

Civil Engineering Institute (I-14), Wrocław University of Technology, Wyb. Wyspianskiego 27, 50-370 Wrocław, Poland

(Received August 13, 2008, Accepted August 17, 2009)

Abstract. In the literature the problem of the topology optimization of the structure is usually solved for one, clearly described from the mechanical point of view material. Generally the topology optimization answers the question of the distribution of this mentioned above material within the design domain. Finally, material-voids distribution it is obtained. In this paper, for the structure mainly strengthened or sometimes weakened by the inclusions, the variation approach of the topology optimization problem is formulated. This multi material approach may be useful for the design process of various mechanical or civil engineering structures which need to be more ”refined” and more “optimal” than they can be using previous topology optimization procedures of optimization one material structures.

Keywords: topology optimization; minimum compliance approach; strengthened structure; multi material structure; mass constraints; FEM.

1. Introduction

This paper is generally based on (in alphabetic order) (Allaire 2002, Bendsøe 1989, Ramm *et al.* 1994, Rozvany *et al.* 1992), and additionally on (Kutyłowski 2000, 2002), where the topology optimization problem is usually considered as one material optimization process which means that finally in each design point of the structure we have the same material properties. Two material models for such continuous material are usually taken into consideration:

– homogenized model
– microstructure model

Homogenized model is shown in Fig. 1(a), where the mass of the continuum structure is homogenized over the entire structure (continuum, homogeneous material is considered). In Fig. 1(b) one can find the example of the microstructure model. In this case even homogenized over the structure material is the material with microstructure. In both cases the same homogeneous material or material with microstructure is used in final optimal topology. This means the optimal topology of considered structure designed within the design domain is obtained for only one kind of material. In other words, finally, in each design point we have the same material properties. As the examples of the real structures we can find (Taylor 2002), where the bridge topology was obtained and we can see (Bendsøe and Sigmund 2003), where many examples of the large scale or microscale

† Professor, E-mail: ryszard.kutylowski@pwr.wroc.pl

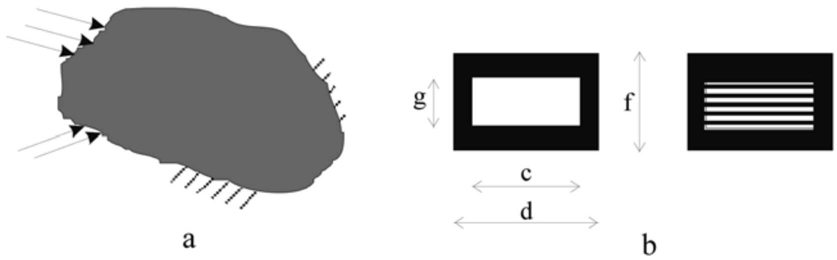

Fig. 1 Homogenized model (a) microstructure model of material (b)

mechanical applications were shown (cars body, micromechanisms and others). Based on (Kutyłowski 2000 and 2002) fast topology optimization procedure is completed to be able obtained optimal topology with inclusions.

Let us consider another structures made of the material characterized by more than one mechanical property. This research was inspirited by the human bone structure which is made of, we can say one material (bone material), but characterized by various mechanical properties if we go from one material point to another material point of the bone. This means, the bone is made of many materials. The density of the bone and Young's modulus of the bone are changing from place to place and they are proper to carry the load of the body. For this case bone properties are provided by the experiments and they can be compared with theoretical models using for example two phases homogenization (Hellmich 2003).

In this paper we will try to exam the structures with inclusions which can be stronger or weaker than the basic material. In other words the multi material structures will be considered to obtain the optimal topology. Such stated problem has no so many examples in literature, because word *multimaterial* usually means mixture of materials or laminated material, for example see (Bendsøe and Sigmund 2003) or composite material see (Belytschko *et al.* 2003) where for example in Fig. 7 it is shown Huber - von Mises stress distribution for final design and it is clear that in some design domains the material properties should be changed.

Based on this analysis it seems that it is better the structure is made of more than one material. Sometimes it is worth speeding up the optimization process. This can be done by imposing during this process in more stressed domains stronger material than it can be stated by usual optimization process. This can be called as artificial strengthening of the structure.

Imposing inclusions into the optimized structure seems to be very necessary because of specific requirement of special structural cases which can be used in mechanical structures, civil engineering structures, and especially in micromechanical structures. Good example how we can make the structure more resistant on cracks is presented in (Guan 2005), where it is shown that design process leads into the topology in which cracks can arise in proper places where the structure is ready to be enough strong to be resistant to them. Additionally the material is removed from the domains where crack can destroy the structure. When we try to analyse the bars we can see that along cracks lines the bars are thicker. They can be thinner when we impose inclusion along the bar which make the bars stronger. The sense of making the structure stiffer or weaker in some domains can be understood analyzing the example of dampers for seismic response control (Desu *et al.* 2007). Instead of continuous one material topology in (Zhou and Wang 2007) one can find three materials topology optimization approach, which leads to distribution of hard, soft and softer materials. The quantity of these materials used in optimal topology is comparable. Saxena (2005) proposed optimal topology of compliant mechanisms as the structure made of various material, but each bar is made of one material (genetic algorithm procedure and the large displacements theory mechanisms). In (Yin and Ananthasuresh 2001) similar to the previous paper two materials topology optimization is discussed. Additionally authors show the example where in some design points flexible material is distributed for optimal topology. This proves that imposing the inclusions is very effective and improves the topology. As it can be seen in the literature two or more materials topology optimization means bars made of one kind of material, but the structure is made of two or more bar kinds. There is the shortage of examples of locally imposing inclusions which can make the structure locally stronger or weaker.

In proposed in this paper approach the quantity of inclusions (stronger or weaker) is very small and the inclusions are discrete distributed. Some examples which show that proposed approach is useful and it is needed for designing process are mentioned below. How to do that is using examples shown in chapter 3.

The paper consists of theoretical background and based on FEM numerical analysis, which illustrates the special features of proposed approach. There were chosen very simple examples to show considered problem and to compare with earlier presented examples for one material. The main goal is to discuss the problem, not analyzing complicated examples. Presented idea mainly may be useful in e.g. new generation of the artificial bone (prosthesis) or in micromechanical systems. In these cases the professional numerical codes are required for every problem separately. They can be based on some parts of the discussion made here. It seems that the commercial professional systems may be completed by the special interfaces based on proposed hints.

The following assumptions are made for considered problem:

- The minimum compliance approach is used with the constraints put on the mass of the structure
- The stress (the strain energy) analysis of the design points of the structure for succeeding optimization steps is the base of the topology optimization algorithm
- Young's modulus updating algorithm separately for each design point is implemented as the core of the topology optimization procedure
- The designer may decide (and the procedure is also able) to make stronger (or weaker) chosen design point. This let design various needed optimal structures and may be useful for the fast procedures which should show the estimated topology needed for the final designing

2. Theoretical background

Minimum compliance material continuum topology optimization problem is considered in this paper. It is stated in variational form. A functional defining the compliance of a structure including proper terms connected together with the compliance of inclusions under constraints imposed on its body mass is minimized.

The first step is the homogenization the available mass within the entire design domain. Solving the boundary problem we can obtain the solution of it, finding the unique vector of the displacement. The mean compliance of the structure, defined below, is the reciprocal to the stiffness of the structure

$$\Pi^E(x, v) = \int_{\Omega} \rho(x) b^i v_i d\Omega + \int_{\partial\Omega_t} t^i v_i ds \tag{1}$$

where $\rho(x)b^i$ is the component of the body forces, v^i is the component of the displacement field and t^i is the component of the traction force. The objective is defined as the total strain energy which is an equivalent to the mean compliance of the structure

$$\Pi^E(x,v) = \Pi^I(x,v) \tag{2}$$

where

$$\Pi^I(x,v) = \frac{1}{2}\int_\Omega C^{ijkl}(x,v,\rho(x))e_{ij}(v)e_{kl}(v)d\Omega \tag{3}$$

During the optimization process the available mass (m_0) is distributed within fixed design domain

$$m_0 = \alpha m, \quad 0<\alpha<1 \tag{4}$$

where α is the mass reduction coefficient, m is the mass which fulfill the entire design domain representing by the volume V of the design domain Ω

$$m = V\rho \tag{5}$$

For homogenized structure the objective functional is defined

$$F(\rho(x),\lambda) = \int_\Omega C^{iklm}(\rho(x))e_{ik}e_{lm}d\Omega + \lambda\Big(\int_\Omega \rho_h d\Omega - m_0\Big) \tag{6}$$

where ρ_h is a density of the homogenized design domain fulfill by the available mass and λ is the Lagrangre multiplier. Elasticity tensor C^{ijkl} is a function of Young's modulus

$$C^{ijkl} = C^{ijkl}(E(\rho(x))) \tag{7}$$

The following constraints are put on the mass of the structure during optimization process

$$H(\rho_j) = \frac{m_j}{m_0} - 1 = 0 \tag{8}$$

what can be understood as follow: the mass of the structure in the j-step of optimization is equal to the available mass. The objective functional (6) taking into account the inclusions and the constraints put on the mass of the structure during the optimization process should be reformulated into the form

$$\begin{aligned} F(\rho(x),\gamma(x),\eta(x),\lambda^m,\lambda^v,\lambda^d) &= \int_\Omega C^{iklm}(\rho(x))e_{ik}e_{lm}d\Omega_m + \int_{\Omega_d} C_d^{iklm}(\gamma(x))e_{ik}e_{lm}d\Omega_m + \\ &+ \int_{\Omega_v} C_d^{iklm}(\eta(x))e_{ik}e_{lm}d\Omega_v + \lambda^m\Big(\int_{\Omega_m}\rho(x)d\Omega_m - m_{0\_\Omega_m}\Big) + \\ &+ \lambda^v\Big(\int_{\Omega_v}\eta(x)d\Omega_v - m_{0\_\Omega v}\Big) + \lambda^d\Big(\int_{\Omega_d}\gamma(x)d\Omega_d - m_{0\_\Omega_d}\Big) \end{aligned} \tag{9}$$

where $\gamma(x)$ is the density in the region where Young's modulus have changed and $\eta(x)$ is the density of voids regions. C_d^{iklm} and C_v^{iklm} are the elasticity tensors of mentioned above regions respectively, and C^{iklm} is the elasticity tensor for material with the density ρ. In the above equation each considered region may consist of many separate subdomains. Searching for the stationary point of the above functional, we obtain the equations which describe considered problem. Because of completing the objective functional by some additional terms connected together with inclusions, minimazing it, following additional equations are obtained

$$\frac{\partial F}{\partial \gamma} = 0 \Rightarrow \frac{\partial (C_d^{iklm}(\gamma(x)) e_{ik}\, e_{lm})}{\partial \gamma} + \lambda^d = 0\,,$$

$$\frac{\partial F}{\partial \lambda^d} = 0 \Rightarrow \int_{\Omega_d} \gamma(x) d\Omega_d = m_{0\_\Omega_d} \tag{10}$$

The mass of Ω regions fulfils the equation

$$m_0 = m_{0\_\Omega_m} + m_{0\_\Omega_v} + m_{0\_\Omega_d} \tag{11}$$

which means: the total sum of the mass of the structure is equal to the available mass and it is a sum of the mass in all regions (Ω_m, Ω_v, Ω_d) within the design domain Ω.

3. FEM examples

The finite element analysis consists of two base topics:
1. Initial estimation of the topology
2. Improvement of the topology optimization techniques which includes:
– Artificial material strengthening
– Strengthening more strenuous elements
– Assuming the position of material elements (applying for compliant mechanisms)

The above problems require using inclusions. Imposing these inclusions we can change one material structure into multi material structure.

The cantilever beam example is presented as the benchmark example (Fig. 2), which can be compared with the literature. Black and white with the shades of grey or 1/0 with numbers in the range from 0 to 1 there are two notations which are used to show the material distribution within the design domain in the next figures. Black and 1 indicate the initial density of material. The shades of grey and the numbers belonging to the open range 0 to 1 indicate the material with relatively smaller density. The results presented here are considered only from the qualitative point of view, the material data and dimensions are given as dimensionless.

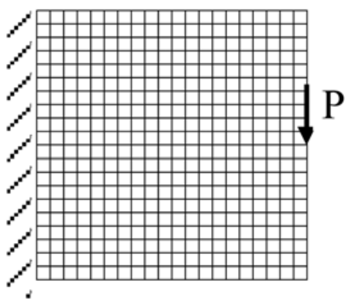

Fig. 2 Benchmark example with 20×20 FE mesh

3.1 Initial topology estimation

In many topology optimization courses we want to know the rough topology at the beginning. In other words sometimes we need to estimate the topology. This can be useful to prepare the exact procedures which are able to find refined topology in normal topology optimization course.

The most important problem in this fast estimation of optimal topology is to find out the general topology which means we should indicate the main bars (connections) within the material design domain. How to do that? We should prepare an interactive procedure which can recognize the most stressed domains, what in other words means, that this procedure is able to answer the question concerning the problem which elements finally should be fulfil by material or not. It can be prepared into self-contained work or sometimes it can be controlled by the designer during the optimization process.

In the case of simply topologies the procedure can recognize even in the first or second step more strenuous domains. After this recognizing the procedure is able to indicate the most probable structure shape, which can be interpreted as the most probable structure topology. Just after recognizing the most stressed domains the procedure imposes stronger material into the finite elements which correspond to these most stressed domains. This process is compatible with the formulation of the problem from the section 2. The explanation of proposed idea is shown using previous presented example (Kutyłowski 2002) which is shown in Fig. 3 (for the mesh shown in Fig. 2) where on the right there is the 0/1 topology for 14th step and on the left there is the previous (13th) step with some shades of grey. The details concerning the optimization parameters used for improved topology optimization procedure are stated in the next chapter.

Fig. 4 shows in number mode the topologies since first to fourteenth step. It can be seen how the mass is moving during the optimization process. This analysis may be fruitful for organizing the procedure for initial topology estimation.

Let start to describe how the procedure works. Tracing the procedure algorithm we should try to analyse the topology of the first optimization step which is shown in Fig. 5. The analysis will be done for successive cross sections numbered in vertical direction since 1 to 20 in Fig. 5. These cross sections numbers for easier identifying are written above the design domain. Additionally in this figure the final optimal topology for 14th step is marked by the shade of grey. Analysing the topology in Fig. 5 it is seen that more stressed elements with greater material density creates the final topology. Only some elements with relatively greater density placed in the cross sections since 11 to 16 above and below the main bars in optimal topology become voids. On the other hand some elements with relatively smaller density become material elements (with the density equal to 1) in

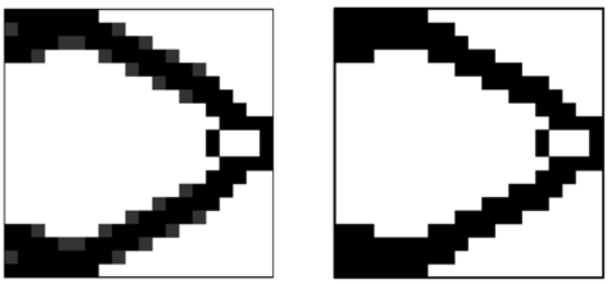

a b

Fig. 3 The base example 13th step (a), 14th step (b)

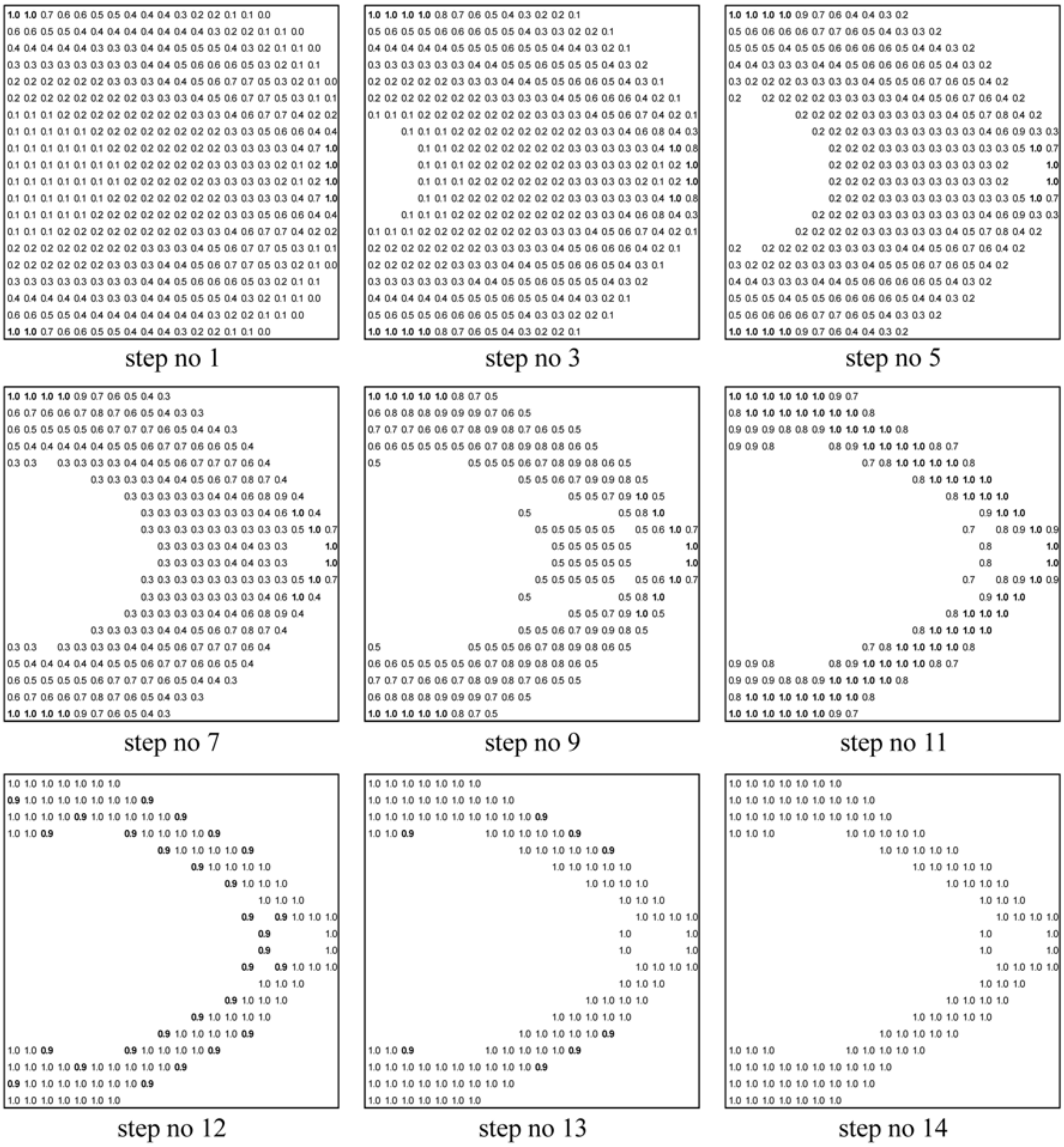

Fig. 4 Topologies since first to fourteenth step

the cross sections since 1 to 9. It is very interesting that in the first optimization step a large majority of elements are recognized by the optimization procedure properly and they have relatively greater density. The initial estimations procedure is able to indicate these elements belonging to the final optimal topology (Fig. 5, elements marked by the shade of grey). Some details how this procedure works is described below.

For considered example (cantilever beam problem) the element density analysis (equivalent of the element strain energy analysis) can be done for each of 20 cross sections separately. Fig. 6 shows

1	2	3	4	5	6	7	8	9	10	11	12	13	14	15	16	17	18	19	20
1,000	0,951	0,743	0,649	0,590	0,539	0,492	0,447	0,401	0,350	0,294	0,234	0,172	0,115	0,071	0,043				
0,603	0,628	0,536	0,471	0,424	0,391	0,368	0,356	0,353	0,358	0,361	0,350	0,311	0,239	0,156	0,090	0,051	0,032		
0,406	0,423	0,413	0,380	0,352	0,334	0,330	0,340	0,368	0,412	0,462	0,500	0,495	0,426	0,308	0,187	0,100	0,053	0,032	
0,296	0,307	0,311	0,304	0,294	0,289	0,296	0,317	0,357	0,418	0,495	0,573	0,624	0,608	0,506	0,347	0,195	0,098	0,051	
0,216	0,226	0,236	0,241	0,243	0,246	0,256	0,277	0,312	0,366	0,440	0,532	0,627	0,693	0,679	0,546	0,343	0,175	0,086	0,045
0,159	0,170	0,183	0,193	0,200	0,208	0,217	0,232	0,254	0,288	0,337	0,408	0,504	0,617	0,709	0,704	0,521	0,285	0,144	0,081
0,120	0,131	0,145	0,158	0,168	0,177	0,186	0,196	0,207	0,223	0,247	0,283	0,340	0,430	0,555	0,676	0,684	0,430	0,240	0,165
0,094	0,106	0,120	0,134	0,146	0,156	0,165	0,173	0,181	0,190	0,202	0,218	0,241	0,279	0,348	0,465	0,604	0,641	0,410	0,383
0,078	0,090	0,104	0,118	0,131	0,142	0,152	0,162	0,172	0,184	0,198	0,215	0,234	0,250	0,263	0,281	0,342	0,449	0,651	1,000
0,070	0,083	0,097	0,111	0,124	0,136	0,147	0,158	0,171	0,187	0,208	0,236	0,267	0,295	0,304	0,274	0,207	0,148	0,168	1,000
0,070	0,083	0,097	0,111	0,124	0,136	0,147	0,158	0,171	0,187	0,208	0,236	0,267	0,295	0,304	0,274	0,207	0,148	0,168	1,000
0,078	0,090	0,104	0,118	0,131	0,142	0,152	0,162	0,172	0,184	0,198	0,215	0,234	0,250	0,263	0,281	0,342	0,449	0,651	1,000
0,094	0,106	0,120	0,134	0,146	0,156	0,165	0,173	0,181	0,190	0,202	0,218	0,241	0,279	0,348	0,465	0,604	0,641	0,410	0,383
0,120	0,131	0,145	0,158	0,168	0,177	0,186	0,196	0,207	0,223	0,247	0,283	0,340	0,430	0,555	0,676	0,684	0,430	0,240	0,165
0,159	0,170	0,183	0,193	0,200	0,208	0,217	0,232	0,254	0,288	0,337	0,408	0,504	0,617	0,709	0,704	0,521	0,285	0,144	0,081
0,216	0,226	0,236	0,241	0,243	0,246	0,256	0,277	0,312	0,366	0,440	0,532	0,627	0,693	0,679	0,546	0,343	0,175	0,086	0,045
0,296	0,307	0,311	0,304	0,294	0,289	0,296	0,317	0,357	0,418	0,495	0,573	0,624	0,608	0,506	0,347	0,195	0,098	0,051	
0,406	0,423	0,413	0,380	0,352	0,334	0,330	0,340	0,368	0,412	0,462	0,500	0,495	0,426	0,308	0,187	0,100	0,053	0,032	
0,603	0,628	0,536	0,471	0,424	0,391	0,368	0,356	0,353	0,358	0,361	0,350	0,311	0,239	0,156	0,090	0,051	0,032		
1,000	0,951	0,743	0,649	0,590	0,539	0,492	0,447	0,401	0,350	0,294	0,234	0,172	0,115	0,071	0,043				

Fig. 5 First optimization step in number mode with 14th step marked by the shade of grey

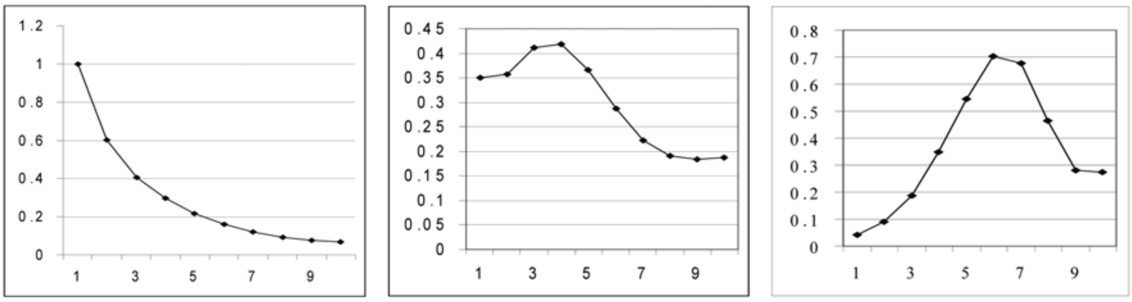

a b c

Fig. 6 The densities from Fig. 5 for 1st cross section (a), 10th cross section (b), 16th cross section (c)

some selected density charts (vertical axis) for the first, tenth and sixteenth cross sections. These charts were drawn for 10 elements (the structure has the horizontal axis) taken from the top to the cantilever beam symmetry axis. As an example in Fig. 6(a) the density for successive elements is as follow: 1.0, 0.6, 0.4, and so on.

The analysis of the density distribution during the optimization process is very important in this research. Base on this, it is clear that most elements with the density in the range 0.3 to 1 or in the range 0.4 to 1 in the first optimization step belong to the set of material elements (density equal to 1) of the final optimal step (Fig. 5 - shade of grey elements). The procedure estimates the above boundary density level. This estimation is mainly based on proper bar thickness, which is equal to 120/20=6=2×3, because the available mass is equal to 120 for the mass reduction coefficient α equal to 0.3 (400 elements×0.3=120). We have 20 cross sections and each cross section is dividing into two bars. Tracing the density level in all the elements the procedure can recognize the topology with the mean bar thickness equal to 3 (which means the bar thickness may changes since 2 to 4 elements).

Additionally the algorithm takes into account the structure load. As the example of it let analyse the cross section number 10 (Fig. 5 and Fig. 6(b)): going from the top, five elements have the

1	2	3	4	5	6	7	8	9	10	11	12	13	14	15	16	17	18	19	20
1	1	1	1	1	1	1	1	1	0,35	0,29	0,23	0,17	0,12	0,07	0,04				
1	1	1	1	1	0,39	0,37	0,36	0,35	0,36	0,36	0,35	0,31	0,24	0,16	0,09	0,05	0,03		
1	1	1	0,38	0,35	0,33	0,33	0,34	0,37	1	1	1	1	1	0,31	0,19	0,10	0,05	0,03	
0,30	0,31	0,31	0,30	0,29	0,29	0,30	0,32	0,36	1	1	1	1	1	1,00	0,35	0,20	0,10	0,05	
0,22	0,23	0,24	0,24	0,24	0,25	0,26	0,28	0,31	0,37	1	1	1	1	1	1	0,34	0,18	0,09	0,05
0,16	0,17	0,18	0,19	0,20	0,21	0,22	0,23	0,25	0,29	0,34	1	1	1	1	1	1	0,29	0,14	0,08
0,12	0,13	0,15	0,16	0,17	0,18	0,19	0,20	0,21	0,22	0,25	0,28	0,34	1	1	1	1	1	0,24	0,17
0,09	0,11	0,12	0,13	0,15	0,16	0,17	0,17	0,18	0,19	0,20	0,22	0,24	0,28	0,35	1	1	1	1	0,38
0,08	0,09	0,10	0,12	0,13	0,14	0,15	0,16	0,17	0,18	0,20	0,22	0,23	0,25	0,26	0,28	0,34	1	1	1
0,07	0,08	0,10	0,11	0,12	0,14	0,15	0,16	0,17	0,19	0,21	0,24	0,27	0,30	0,30	0,27	0,21	0,15	0,17	1
0,07	0,08	0,10	0,11	0,12	0,14	0,15	0,16	0,17	0,19	0,21	0,24	0,27	0,30	0,30	0,27	0,21	0,15	0,17	1
0,08	0,09	0,10	0,12	0,13	0,14	0,15	0,16	0,17	0,18	0,20	0,22	0,23	0,25	0,26	0,28	0,34	1	1	1
0,09	0,11	0,12	0,13	0,15	0,16	0,17	0,17	0,18	0,19	0,20	0,22	0,24	0,28	0,35	1	1	1	1	0,38
0,12	0,13	0,15	0,16	0,17	0,18	0,19	0,20	0,21	0,22	0,25	0,28	0,34	1	1	1	1	1	0,24	0,17
0,16	0,17	0,18	0,19	0,20	0,21	0,22	0,23	0,25	0,29	0,34	1	1	1	1	1	1	0,29	0,14	0,08
0,22	0,23	0,24	0,24	0,24	0,25	0,26	0,28	0,31	0,37	1	1	1	1	1	1	0,34	0,18	0,09	0,05
0,30	0,31	0,31	0,30	0,29	0,29	0,30	0,32	0,36	1	1	1	1	1	1,00	0,35	0,20	0,10	0,05	
1	1	1	0,38	0,35	0,33	0,33	0,34	0,37	1	1	1	1	1	0,31	0,19	0,10	0,05	0,03	
1	1	1	1	1	0,39	0,37	0,36	0,35	0,36	0,36	0,35	0,31	0,24	0,16	0,09	0,05	0,03		
1	1	1	1	1	1	1	1	1	0,35	0,29	0,23	0,17	0,12	0,07	0,04				

Fig. 7 First optimization step in number mode with 14^{th} step marked by the shade of grey with indicated elements for proposed topology

density greater than 0.3, but the first two elements should be rejected, because the load is in the middle of the right side and this is why the bar should take direction into the load. Finally for this cross section we may take into account next two or three elements. Analysing the cross section number 16, five elements should be indicated for one bar. Unfortunately, at this first optimization step it is impossible to indicate elements which are on the cantilever horizontal symmetry axis, because they have too small density (0.27 for cross section number 16). When we assume to the algorithm the boundary value equal to 0.4 we can obtain the distribution shown in Fig. 7. Indicated elements are marked by "1". This boundary value can be understood as the boundary value of the density and the elements with the density greater than this boundary value will be indicated as belonging to the probably optimal topology. Unfortunately this automatic indication does not take into account the above analysis concerning neglecting the elements which are above the upper bar and below the lower bar in the cross sections number 8, 9 and since number 11 to 17 or even to number 18 (these elements which are not belonging to the shade of grey background). Additionally we should neglect most of these elements because with them the total elements number in some cross sections exceeded mentioned above the mean number equal to 6. From one point of view the procedure is based on the above hints, but on the other hand when the algorithm has indicated too many elements in some cross sections, to relocate the mass the special procedure should be activated. It is described below.

The algorithm is checking the bar thickness and it is able to relocate the mass from these elements which are below and above the main two bars. Because of the structure load the mass should be closer to the horizontal symmetry axis. Additionally, the algorithm is checking the mean bar thickness (three elements of one bar in this case). The mass removing from the elements placed below and above the main two bars is moving mainly into these elements which were not indicated (not marked by "1"). These elements have the density below the boundary level equal to 0.4, but close to it (in the range 0.3 to 0.4). They are placed mainly in 6^{th} to 10^{th} cross sections. The algorithm is finding such elements checking the elements density in successive cross sections. It takes into account the elements with relatively greater density. In the 8^{th} and 9^{th} cross sections the maximum elements density is between 0.32 and 0.37 (maximum 3 elements). When it is enough free mass after the above moving, the procedure should try to connect the main two bars as it was made by optimization process (step number 14) in cross section number 16 (elements with the

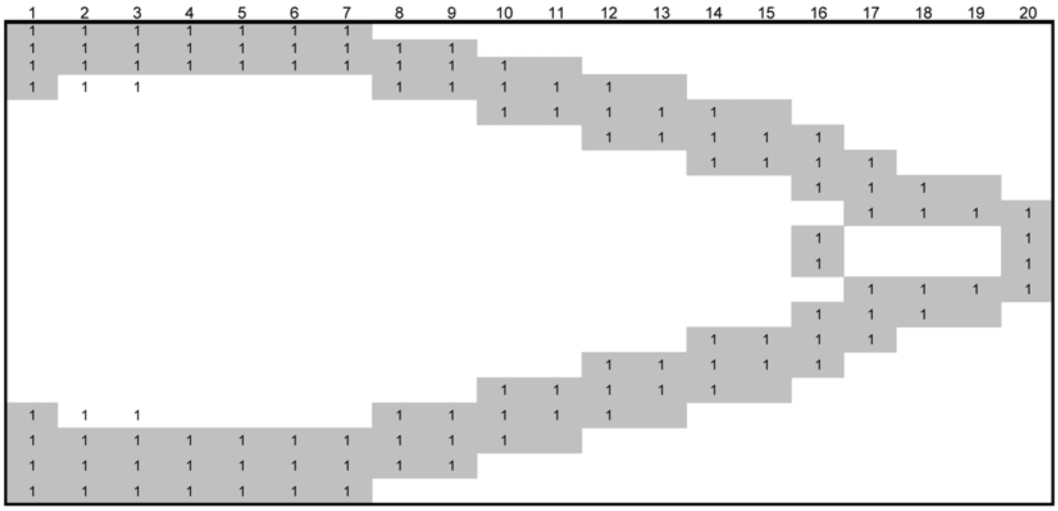

Fig. 8 Topology for 14^{th} step marked by “1” and estimated topology marked by the shade of grey

density equal to 0.27 in Fig. 7). The final topology obtained using proposed procedure is shown in Fig. 8 where in number mode it is the final topology (14^{th} step - 0/1 distribution - Fig. 3(b)) and marked by the shade of grey the estimated optimal topology using proposed procedure are shown. The total mass for this shade of grey topology is equal to 118 and it is closer to the available mass equal to 120 and more than for 14^{th} step for which the mass is equal to 114. As it can be seen 4 elements belonging to the 14^{th} step topology (placed near the left edge) were not indicated as the proper elements for the estimated topology. Using postprocessing, two elements will be fulfil by material and the mass will be equal to the available mass.

Information concerning the total mass mentioned above, discussed in below tables and in some below figures should be interpreted as follow: Eqs. (8) and (11) are valid for successive optimization steps during the optimization process. Sometimes we can reach optimum solution holds these equations, sometimes the procedure near the minimum strain energy solution indicates that minimum strain energy solution is obtained for less mass than available mass was assumed. This means the optimal solution needs less mass and the postprocessing is needed to complete the mass in case if this mass must be completed from the other reasons.

In case when the procedure assumes the boundary value equal to 0.3, too many elements are indicated and based on such indication it is not easy to predict real optimal topology. The procedure works as follow: when too many elements are indicated the procedure enlarges the boundary value (into 0.4 in this case).

Considered procedure let estimate the optimal topology or additionally using the postprocessing this procedure let obtain the optimal topology.

Sometimes this procedure is not able to indicate the proper topology (when it shows too simply topology for example). The procedure may recognize that within the first step there is not enough information to indicate the final elements properly. In this case it goes to the next step and it is repeated. Even we should make the prediction of the final optimal topology within two or three steps it is faster than using usual procedure for finding the optimal topology what needs many steps.

This procedure is not effective when too many design points have very similar strain energy value level. In such cases we should come back to normal topology optimization procedure and after some steps we are able to recognize more stressed domains. This let us start this recognizing procedure which after analysis more stressed domains can show optimal topology in considered domain. This can be repeated until in the entire design domain we obtain the optimal topology. This procedure is faster than usual used topology optimization procedures and can be useful for initial topology recognizing, for controlling usual procedures, for making the decision concerning selection of needed kind topology optimization procedures.

3.2 Improvement topology optimization techniques

The main goal is to obtain more refined topology with less value of the strain energy. The problem is stated for earlier considered optimization parameters for this example (Kutyłowski 2002). This let us compare the effectiveness of proposed improvement techniques. The base examples are presented for the mass reduction coefficient α equal to 0.3. The threshold functions are defined as

$$TF_1 = 0.1\alpha j$$
$$TF_2 = 0.0125\alpha j \tag{12}$$

where j is the number of current optimization step during optimization process. TF_2 let obtain the more refined topology, but within more optimization steps than it can be done using TF_1. Young's modulus is updating using the equation

$$E = E_0\left(\frac{\rho}{\rho_0}\right)^3 \tag{13}$$

where E_0 is an initial Young's modulus, ρ_0 is an initial density, ρ is a density for $j-1$ step. Young's modulus is updating for each finite element in each optimization step separately. In Fig. 3 the solution for TF_1 is shown. Fig. 9 shows the solution for TF_2 in the same form as it is in Fig. 3 for TF_1.

3.2.1 Artificial material strengthening

The matter consists in artificial material strengthening these finite elements in which the density have achieved the density of the structure material (have achieved "1" when the distribution is

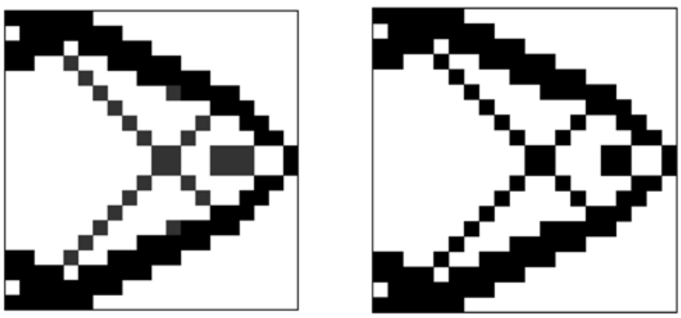

a b

Fig. 9 The example for TF_2 86th step (a), 87th step (b)

Table 1

	TF_1	TF_1	TF_2	TF_2
	13th step	14th step	86th step	87th step
total mass	119.09	114.00	118.78	118.00
strain energy	2.55	2.95	2.39	2.33

Table 2

	TF_1	TF_1	TF_2	TF_2
	13th step	14th step	107th step	108th step
total mass	119.97	118.00	117.90	118.00
strain energy	2.65	2.53	1.98	1.97

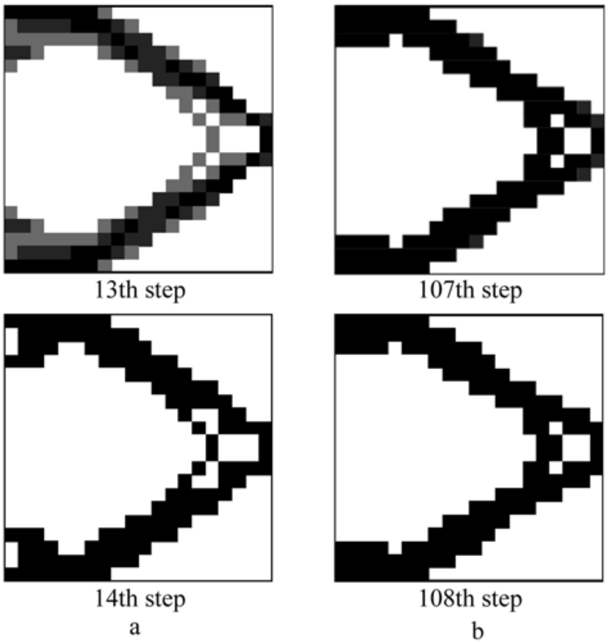

Fig. 10 Artificial ten times material strengthening example for TF_1 (a), TF_2 (b)

considered in number mode). It is made during the optimization process for each optimization step separately. This very simply procedure treatment gives more refined topology. It was assumed ten times material strengthening in this case at the beginning.

Table 1 concerns the results of traditional topology optimization procedure and Table 2 concerns the results of artificial ten times strengthened case. Compared both tables it can be seen that for both threshold functions separately smaller strain energy is obtained for artificial material strengthening procedure. Additionally this energy is generally smaller than it was obtained without using improving procedure. Fig. 10 shows the results of artificial ten times material strengthening example for TF_1 and for TF_2.

To make deeper look into this problem the material strengthening is additionally assumed as two

Table 3

	TF_1	TF_1	TF_2	TF_2
	Two times			
	12^{th} step	13^{th} step	77^{th} step	78^{th} step
total mass	119.89	118.00	117.89	114.00
strain energy	3.51	3.06	2.44	2.43
	Fifty times			
	12^{th} step	13^{th} step	99^{th} step	100^{th} step
total mass	119.89	118.00	118.21	116.00
strain energy	2.63	2.51	2.25	2.23
	One hundred times			
	13^{th} step	14^{th} step	103^{th} step	104^{th} step
total mass	119.97	118.00	117.00	114.00
strain energy	2.62	2.50	2.10	2.09

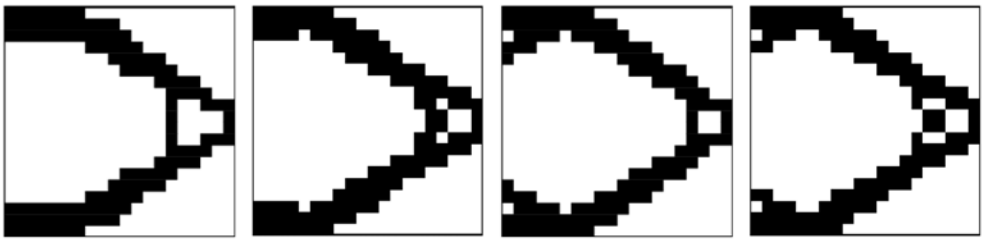

2 times, 78th step   10 times, 108th step   50 times, 100th step   100 times, 104th step

Fig. 11 Artificial material strengthened examples for TF_1

times, fifty times and one hundred times strengthening. The results are presented in the Table 3 and in Fig. 11.

The topologies and the strain energy for TF_1 are very similar except the example where the material is strengthening two times (Table 2 and Table 3). For TF_2 the smallest strain energy is for ten times the material strengthening (Fig. 10 and Fig. 11). It is clear, the optimal solution may be obtained depending on the topology optimization steering parameters. This analysis shows how difficult is to find proper optimization path.

3.2.2 Strengthening more strenuous elements

It is very interesting how the topology changes when some more strenuous elements are strengthened. In the human bone the most stressed bone domains are stronger than other domains. This let make the structure of human bone system more optimal. In our solution based on the optimization process analysis we are able to indicate which elements are more stressed. They are usually these elements which firstly create the bar. In other words they are the bar core.

$\boxed{1.000}$	1.000	1.000	1.000	0.947	0.764	0.597	0.472	0.382											
0.575	0.710	0.675	0.687	0.759	0.810	0.774	0.666	0.540	0.435	0.360									
0.603	0.574	0.556	0.517	0.531	0.606	0.705	0.770	0.755	0.663	0.546	0.454	0.390							
0.513	0.458	0.421	0.396	0.401	0.433	0.492	0.575	0.675	$\boxed{0.755}$	0.758	0.679	0.572	0.472	0.377					
0.375					0.353	0.380	0.412	0.461	0.539	0.649	$\boxed{0.749}$	0.778	0.711	0.573	0.411				
						0.346	0.355	0.366	0.385	0.424	0.500	0.622	0.758	0.827	0.729	0.424			
							0.345	0.347	0.350	0.355	0.364	0.390	0.462	0.611	0.823	0.934	0.406		
								0.349	0.351	0.357	0.359	0.356	0.352	0.369	0.451	$\boxed{0.678}$	1.000	0.380	
										0.360	0.371	0.374	0.373	0.363		0.369	0.504	1.000	0.676
										0.359	0.375	0.387	0.393	0.393	0.381				$\boxed{1.000}$
										0.359	0.375	0.387	0.393	0.393	0.381				$\boxed{1.000}$
										0.360	0.371	0.374	0.373	0.363		0.369	0.504	1.000	0.676
								0.349	0.351	0.357	0.359	0.356	0.352	0.369	0.451	$\boxed{0.678}$	1.000	0.380	
							0.345	0.347	0.350	0.355	0.364	0.390	0.462	0.611	0.823	0.934	0.406		
						0.346	0.355	0.366	0.385	0.424	0.500	0.622	0.758	0.827	0.729	0.424			
0.375					0.353	0.380	0.412	0.461	0.539	0.649	$\boxed{0.749}$	0.778	0.711	0.573	0.411				
0.513	0.458	0.421	0.396	0.401	0.433	0.492	0.575	0.675	$\boxed{0.755}$	0.758	0.679	0.572	0.472	0.377					
0.603	0.574	0.556	0.517	0.531	0.606	0.705	0.770	0.755	0.663	0.546	0.454	0.390							
0.575	0.710	0.675	0.687	0.759	0.810	0.774	0.666	0.540	0.435	0.360									
$\boxed{1.000}$	1.000	1.000	1.000	0.947	0.764	0.597	0.472	0.382											

Fig. 12 Topology for 8^{th} step with chosen for strengthening elements

Used here procedure consists of two parts:

1. Indication of the elements which should be strengthened.
2. Finding out the optimal topology for initially strengthened structure.

Mentioned above the first part is extended usual optimization procedure. This extension consists in:

– finding out the more stressed elements during usual optimization course for each step,
– comparing the element effort for successive optimization steps,
– indication of these elements which should be strengthened.

As an example (8^{th} step) in Fig. 12 it can be seen marked indicated elements. The number of indicated elements can be generated automatically or can be in designer hands. In this shown here solution the number of finding out most stressed elements was assumed as equal to 10. Four of them (with the density equal to 1) they are the elements near the force P, and at the clamped edge. Four of them were chosen in the middle part of the structure (with the density equal to 0.755 and 0.749). The last two elements (placed closer to the force P with the density equal to 0.678) were indicated as not most stressed elements in fourth cross section counting from the right, but lying near the most stressed elements in the middle of the final bar (see Fig. 3(b) and Fig. 4 for the 14^{th} step). This decision was made based on the load placement (the bar in this case should be closer to the symmetry axis). Considered analysis of the most stressed elements is made during the usual optimization course and it can be stopped when for some successive steps the same elements are indicated.

The second part of considered procedure is usual topology optimization procedure, for which this assumed strengthened for chosen elements, is kept.

In the next two figures (Fig. 13 and Fig. 14) the results for strengthened elements from Fig. 12 are shown. In Fig. 13 the topologies were obtained for TF_1 and in Fig. 14 for TF_2. In each figure in the lower row 0/1 topologies are shown, and in the upper row mainly the previous step with the shades of grey is placed. To have the possibility of comparison in Fig. 13(a) and in Fig. 14(a) earlier mentioned base topologies are shown. The topologies strengthened in ten elements twice and ten times are put in both figures in columns b and c respectively.

We should make the analysis of the lower row pictures in Fig. 13 and in Fig. 14. In Fig. 13 the topologies for b and c cases (2 times and 10 times strengthened respectively) are the same, but the strain energy is lower for 10 times strengthened what is obvious. In Fig. 14 the same analysis gives the same conclusion concerning the strain energy, but the topologies are not the same, they are

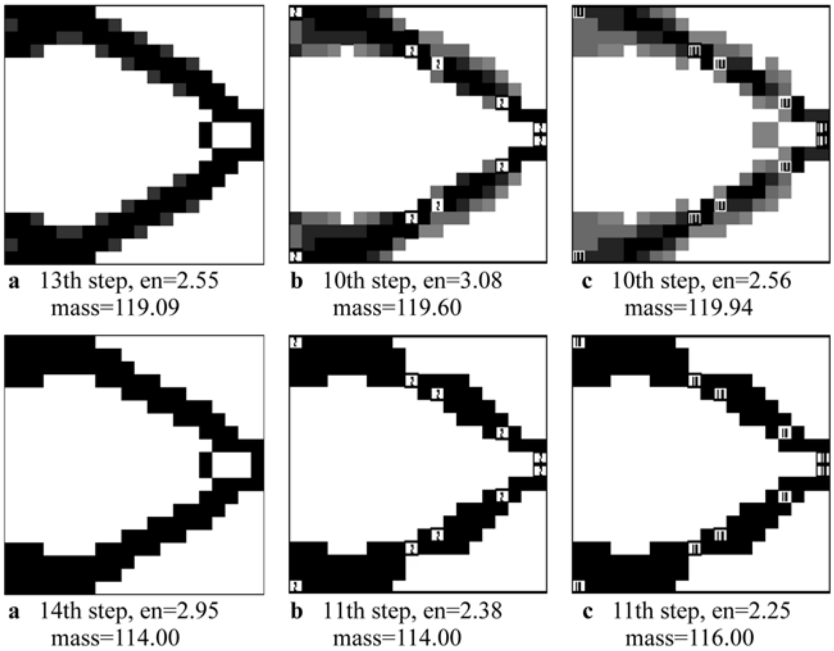

Fig. 13 Topologies for TF_1: the base example (a), 2 times strengthened (b), 10 times strengthened (c)

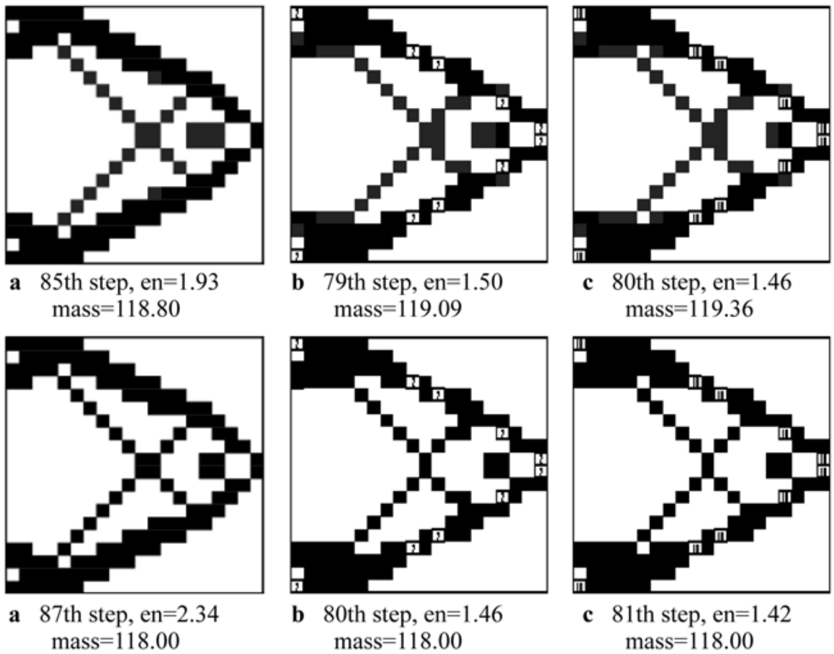

Fig. 14 Topologies for TF_2: the base example (a), 2 times strengthened (b), 10 times strengthened (c)

similar. Placing more strengthened material we are able to change the optimal topology (comparing with the *a* cases in both figures). Obtained topology is "more optimal" because the strain energy is lower after imposing strengthened material. Additionally the bars near the strengthened regions

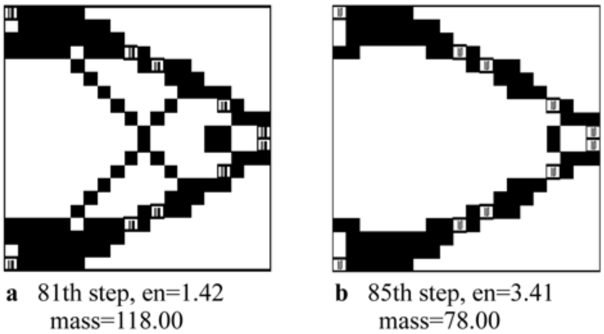

Fig. 15 Topologies for TF_2: the optimal solution (a), the topology obtained for 4 steps later (b)

become thinner. Especially in Fig. 14(b) and in Fig. 14(c) the outer bars are thinner than those in Fig. 14(a).

It is obvious that if the optimization process runs further beyond the optimal solution the strain energy is increasing and the topology becomes weaker what can be seen in Fig. 15 where on the left side it is repeated the picture taken from Fig. 14(c) and on the right side the weak topology obtained within 85 steps is shown. The strain energy increases very rapidly within only 4 steps and the algorithm have cut the inner cross what is the cause of strain energy increasing.

The next example was obtained for the mass reduction coefficient α equal to 0.4 for which the available mass is equal to 160 (Fig. 16). The most of fourteenth strengthened elements were indicated by the procedure as the bars core and the elements with relatively greater density obtained during usual optimization process (Fig. 16(b), (c), (d)). Only two elements for these examples were indicated by the designer. They are placed in the 3^{rd} cross section left from the elements loaded by the force P. This decision was made because of the other design requirements. It is interesting how changes the topology near the left upper and lower corner (Fig. 16(c), (d)). Two stronger elements are enough to carry the load from the structure into the clamped edge. This is the reason of automatic removing the mass from some elements and relocating the mass during the optimization process for five times and ten times strengthened finite elements. In Fig. 16(b) only two times fourteen finite elements were strengthened. As it can be seen the topology generally was changed in comparison with the topology placed in Fig. 16(a). Only in the clamped edge changes are very small. The next two figures (Fig. 16(c), (d)) are identical (comparing the topologies), but the strain energy is a little bit smaller for ten times strengthened case, because stronger elements make the structure stiffer. For all cases the mass for 0/1 distribution is the same (except Fig. 16(b) in which it is similar) and a little bit less than the available mass. Making chosen elements stronger than ten times does not make a sense, because even the differences between the solutions for five and ten times strengthened elements are very small. This examples shows how changes the optimal topology when the designer wants to make stronger some elements because of various design requirements and he runs proposed procedure completing by mentioned above special other design requirements (considering two finite elements).

As another example the structure strengthened not symmetrically in 3 elements is shown in the next two figures in the same system as it is shown in Fig. 13 and in Fig. 14.

In both figures as *a* examples there are the base examples to make easy comparison how changes the topology when we not symmetrically impose strengthened elements in *b* and in *c* examples. It is not possible to obtain 0/1 optimal topology when we use elements two times strengthened only. The

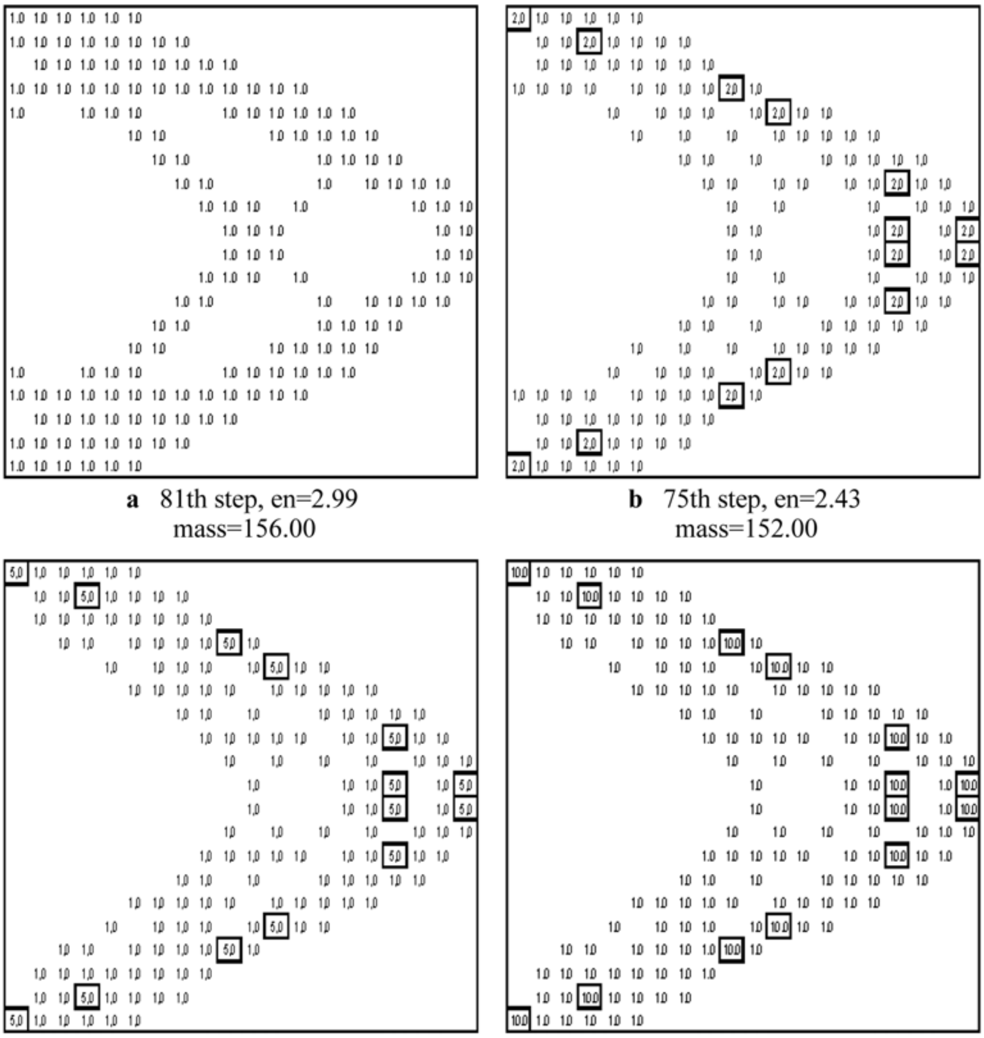

a 81th step, en=2.99 mass=156.00

b 75th step, en=2.43 mass=152.00

c 78th step, en=2.05 mass=156.00

d 78th step, en=2.03 mass=156.00

Fig. 16 Topologies for TF_2 and α=0.4: the base optimal solution (a), the optimal topology obtained for 2 times strengthened (b), the optimal topology obtained for 5 times strengthened (c), the optimal topology obtained for 10 times strengthened (d)

strain energy in this case increased to 3.29 value (0/1 distribution) from 2.47 value for the previous step (Fig. 17(b)). The additional bar constructed for 11^{th} step is unfortunately cut during 12^{th} step. This is the reason of increasing the strain energy. This structure is too weak. When we use elements ten times strengthened the situation changes and the smallest strain energy is for 12^{th} step. In this case the additional bar (needed for Fig. 17(b) case) is not required, probably because ten times strengthened elements make the upper bar enough strong to carry the load. The lower bar in *b* and in *c* cases is thicker than in *a* case. Upper bar in strengthened domain is thinner, but in other domains is thicker if we compare with *a* case.

In Fig. 18(b) the situation noticed in Fig. 17(b) is repeated. The strain energy for 88^{th} step (0/1

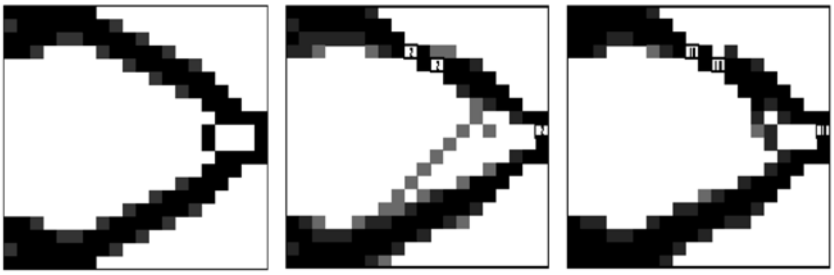

a 13th step, en=2.55 mass=119.09 **b** 11th step, en=2.47 mass=119.62 **c** 11th step, en=2.62 mass=119.37

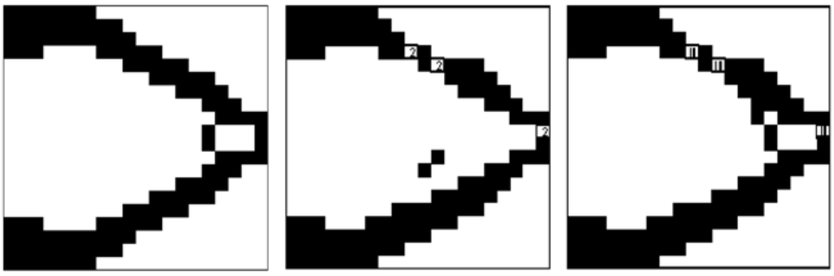

a 14th step, en=2.95 mass=114.00 **b** 12th step, en=3.29 mass=113.00 **c** 12th step, en=2.24 mass=117.00

Fig. 17 Topologies for TF_1 (3 strengthened elements): the base example (a), 2 times strengthened (b), 10 times strengthened (c)

distribution) is greater than for 87^{th} step (case *a*). Additionally, thinner lower bar is disconnected. This is a reason of increasing the strain energy in comparison with 87^{th} step. It can be seen that symmetric solution (Fig. 18(a)) is changing (because of such strengthening structure) into not symmetric state. The topologies in Fig. 18 are more refined in comparison with the topologies placed in Fig. 17, what is obvious because of various threshold functions used in both cases. Additionally the strain energy is smaller for examples shown in Fig. 18 comparing with the strain energy given in Fig. 17.

It is interesting to compare Fig. 13 with Fig. 17 and Fig. 14 with Fig. 18. Generally in the same strengthened regions topologies are very similar, but in other regions they are not the same, because of the strengthened manner of the structure.

In Fig. 13 and in Fig. 14 symmetric problem is shown. It is interesting how the topologies change when strengthened elements are placed in no symmetric manner. The results are shown in Fig. 19 and in Fig. 20, where two times strengthened elements are placed in upper bar and ten times strengthened elements are placed in lower bar. Both figures are organized by the same way: figure *c* shows 0/1 distribution of material, figures *a* and *b* show the previous steps.

Especially in Fig. 19 one can notice that ten times strengthening is a cause of the thinner bar around strengthened elements in comparison with 2 times strengthened elements. As it is seen in Fig. 14(b), (c) in the lower row pictures the strain energy is a little bit greater than the strain energy in Fig. 20(c). Very refined topology shown in Fig. 20(c) gives the lowest value of the strain energy. The same boundary conditions and the same load, but different topologies (Fig. 14(b), (c) lower row pictures, Fig. 18(c) lower row picture and Fig. 20(c)). This means it is worth to find out the optimal topology with various materials. As it can be seen more strengthened one bar in comparison with

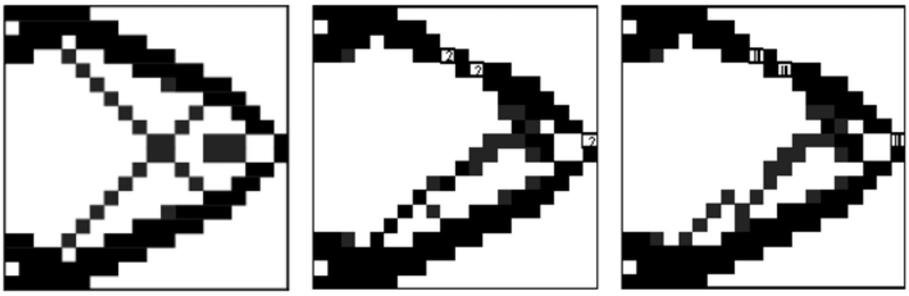

a 85th step, en=1.93 mass=118.80 **b** 87th step, en=1.85 mass=117.60 **c** 86th step, en=1.89 mass=118.60

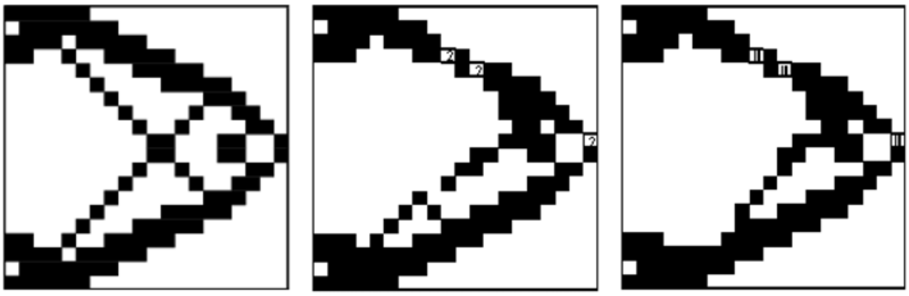

a 87th step, en=2.34 mass=118.00 **b** 88th step, en=2.42 mass=117.00 **c** 87th step, en=1.88 mass=116.00

Fig. 18 Topologies for TF_2 (3 strengthened elements): the base example (a), 2 times strengthened (b), 10 times strengthened (c)

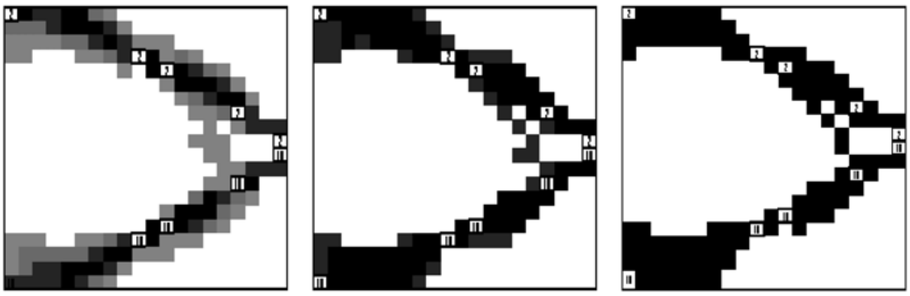

a 10th step, en=2.45 mass=119.98 **b** 11th step, en=1.99 mass=118.99 **c** 12th step, en=1.70 mass=111.00

Fig. 19 Topologies for TF_1

another bar may make the structure stiffer in comparison with the symmetrically strengthened structure (Fig. 19(c) with 13(c), and Fig. 20(c) with Fig. 14(c)).

Let make one change in the above example: in the left upper corner there is a lot material with the density of the initial material (the density equals to 1). In this region we make weaker 4 elements imposing the weak material with the density equal to 0.01. Similar to strengthening material this is kept during the optimization process. Comparing Fig. 20(c) and Fig. 21(b) we can see the change: one short bar rotated around the inner central point of the inner cross to support the weaker region. The strain energy decreased in comparison with the strain energy for topology

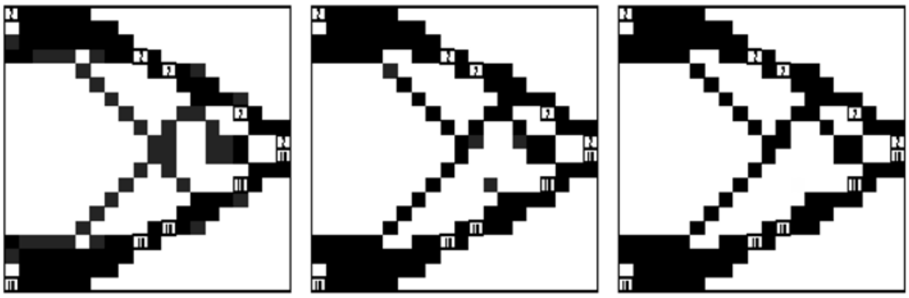

a 76th step, en=1.44 mass=119.10 **b** 79th step, en=1.41 mass=118.20 **c** 80th step, en=1.40 mass=117.00

Fig. 20 Topologies for TF_2

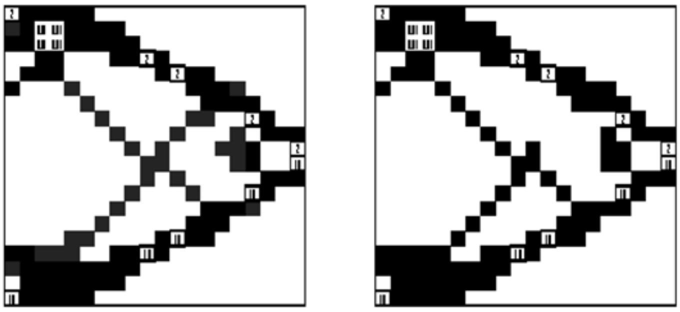

a 77th step, en=1.48 mass=117.0 **b** 81th step, en=1.34 mass=117.0

Fig. 21 Topologies for TF_2 with weak inclusion

shown in Fig. 20(c). Making weaker some regions “more optimal” topology was obtained. This rotated bar made this structure stiffer.

3.2.3 Compliant mechanisms

The above examples were obtained for mainly strengthened material in some elements. In the below example we assume the position of the material elements (with the final density equal to 1) by imposing in some places the load what can be understood as making the supports in the joints. This let us design needed topology which can be useful for various mechanisms, similar to presented in chapter 2.6 in (Bendsøe and Sigmund 2003) and especially in (Yin and Ananthasuresh 2001) where stiffer and weaker materials are distributed within the design domain according to the structural effort. The assumed positions of the additionally loaded elements are marked in Fig. 22 by 4 crosses within the design domain. These elements can be treated as the joints of the structure. Automatically around these elements the mass is distributed. The available mass in Fig. 22(a) was assumed as equal to 120. It was not enough mass to obtain optimal topology. Enlarging the mass to 160 (the mass reduction coefficient α is equal to 0.4) the optimal topology (similar to the topology proposed in Fig. 22(a)) is shown in Fig. 22(b) for the mass equal to 130. This means assumed available mass equal to 160 is too much and assumed available mass equal to 120 is too little to obtain the optimal solution.

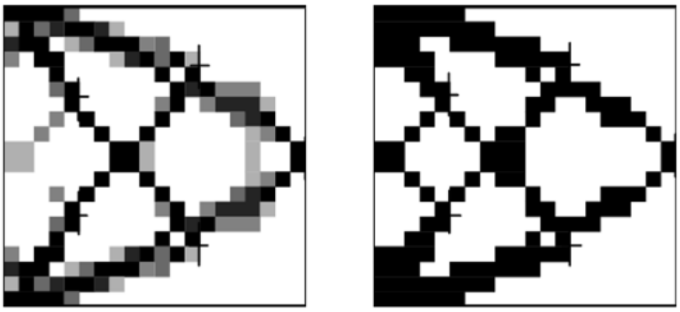

a 77th step, mass=119.8 available mass=120 **b** 84th step, mass=130.0 available mass=160

Fig. 22 Topologies for TF_2

4. Conclusions

The main goal in this research is to make the topology optimization process more efficient (faster and giving the topology characterized by the smaller value of the strain energy). The hints came from this research may be useful for commercial codes for designing special structures (micromechanical or new generation of bone prosthesis for example). One can see how complicated is topology optimization process when various materials are placed at the disposal. The question arises: which material the designer should use for each design point separately? The human bone system is the best example how to design the structure under the changeable load and boundary conditions. These changes are the cause of the variety of the bone property in the bone system within the life time. For the cortical and for the spongy bones Young's modulus is changing many times (especially for the spongy bones) according to the information concerning the structure effort, what is traced in the real life time. This paper tries to open the discussion how the topology optimization procedure should be changed to be useful for optimized in the manner being close to the human bone optimization system.

The analysis of various improvement topology optimization techniques was done for two considered threshold functions. It is clear that it is worth using various improvements procedures e.g. the artificial material strengthening procedure, because they give „more optimal" topology comparing with the topology obtained earlier without new procedures what was discussed in the previous chapter. Improving the material properties in some design points it was possible to observe how the topology changes.

Concluding the following should be expressed:

- Proposed algorithm let obtain the optimal topology of various needed in some cases structures. It is very fast - only a few optimization steps are needed to obtain optimal topology
- It can be observed that imposing to the structure stiffer design points we can obtain more optimal" structure
- Using stiffer or weaker inclusions we obtain multi material structures
- The procedure can be useful in design process (micromechanics structures, bone prosthesis)
- This research gives the general hints for constructing more effective topology optimization procedures

References

Allaire, G. (2002), *Shape Optimization by the Homogenized Method*, Springer, Berlin, Heidelberg, New York.

Belytschko, T., Xiao, S.P. and Parimi, C. (2003), "Topology optimization with implicit functions and regularization", *Int. J. Numer. Meth. Eng.*, **57**, 1177-1196.

Bendsøe, M.P. (1989), "Optimal shape design as a material distribution problem", *Struct. Multidiscip. O.*, **1**, 193-202.

Bendsøe, M.P. and Sigmund, O. (2003), *Topology Optimization, Theory, Methods and Applications*, Springer, Berlin, Heidelberg, New York.

Desu, N.B., Dutta, A. and Deb, S.K. (2007), "Optimal assessment and location of tuned mass dampers for seismic response control of a plan-asymmetrical building", *Struct. Eng. Mech.*, **26**(4), 459-477.

Guan, H. (2005), "Strut-and-tie model of deep beams with web openings - an optimization approach", *Struct. Eng. Mech.*, **19**(4), 361-379.

Hellmich, C., Ulm, F.J. and Dormieux, L. (2003), "Homogenization of bone elasticity based on tissue-independend ('universal') phase properties", *Proc. Appl. Math. Mech.*, **3**, 56-59.

Kutyłowski, R. (2000) "On an effective topology procedure", *Struct. Multidiscip. O.*, **20**, 49-56.

Kutyłowski, R. (2002) "On nonunique solutions in topology optimization", *Struct. Multidiscip. O.*, **23**, 398-403.

Ramm, E., Bletzinger, K.-U., Reitinger, R. and Maute, K. (1994), "The challenge of structural optimization". In: Topping, B.H.V., Papadrakakis, M. (ed) Advanced in Structural Optimization (Int. Conf. on Computational Structures Technology held in Athen), 27-52.

Rozvany, G.I.N., Zhou, M. and Birker, T. (1992), "Generalized shape optimization without homogenization", *Struct. Multidiscip. O.*, **4**, 250-252.

Saxena, A. (2005), "Topology design of large displacement compliant mechanisms withmultiple materials and multiple output ports", *Struct. Multidiscip. O.*, **30**, 477-490.

Taylor, J.E. (2002), "Perspectives on layout and topology design", *Struct. Multidiscip. O.*, **24**, 253-256.

Yin, L. and Ananthasuresh, G.K. (2001), "Topology optimization of compliant mechanisms with multiple materials using a peak function material interpolation scheme", *Struct. Multidiscip. O.*, **23**, 49-62.

Zhou, Z. and Wang, M.Y. (2007), "Multimaterial structural topology optimization with a generalized Cahn-Hilliard model of multiphase transition", *Struct. Multidiscip. O.*, **33**, 89-111.